รหัสโครงการ SUT 7-719-44-12-3

รายงานการวิจัย

Physical properties and the origin of shallow seismic reflectivity, Khorat Basin, NE Thailand

ผู้วิจัย

Dr. Helmut Duerrast

สาขาวิชาเทคโนโลยีธรณี

สำนักวิชาวิศวกรรมศาสตร์

มหาวิทยาลัยเทคโนโลยีสุรนารี

ได้รับทุนอุดหนุนการวิจัยจากมหาวิทยาลัยเทคโนโลยีสุรนารี ปีงบประมาณ พ.ศ. 2544

ผลงานวิจัยเป็นความรับผิดชอบของหัวหน้าโครงการวิจัยแต่เพียงผู้เดียว

มีนาคม 2545

ACKNOWLEDGEMENTS

The principal investigator acknowledges a research grant provided by the Suranaree University of Technology, which made the realisation of this project possible. Many thanks to Mr. Veerayuth Lorprayoon, Ceramic Engineering, Suranaree University of Technology, for his assistance, and to Mr. Keith S. Crosby from the Asia Pacific Potash Corporation in Udon Thani, Thailand, for providing samples for this study.

บทคัดย่อ

จุดประสงค์หลักประการหนึ่งของการสำรวจด้วยวิธีคลื่นสั่นสะเทือน คือเพื่อหาขอบเขตหรือความลึกของชั้นหินในภาคสนามโดยอาศัยหลักการของการสะท้อนกลับของคลื่นระหว่างรอยต่อของหินสองชนิดที่มีคุณสมบัติต่างกัน ขนาดและความกว้างของช่วงคลื่นที่จะนำมาใช้จะถูกกำหนดโดยความต้านทานเสียงสะท้อนของชั้นหิน ซึ่งสามารถคำนวณได้จากความหนาแน่นของชั้นหินคูณด้วยความเร็วของคลื่น แต่ก็สามารถกำหนดด้วยค่าสัมประสิทธิ์ของการสะท้อนได้เช่นกัน ดังสมการข้างล่างนี้

$$R = \frac{\rho_2 V_2 - \rho_1 V_1}{\rho_2 V_2 + \rho_1 V_1} = \frac{Z_2 - Z_1}{Z_2 + Z_1}$$

โดยที่ 1 และ 2 เป็นตัวแทนของหินที่อยู่ชั้นบนและชั้นล่าง ตัวอย่างหินต่างชนิดที่ได้จากชั้นหินในแอ่งโคราชในภาคตะวันออกเฉียงเหนือของประเทศไทย ได้นำมาทดสอบในห้องปฏิบัติการเพื่อหาความหนาแน่นและความเร็วของคลื่นปฐมภูมิและคลื่นทุติภูมิ เพื่อนำผลไปประยุกต์ใช้ประเมินการสะท้อนกลับในระดับตื้นในภาคสนาม จุดประสงค์หลักที่ศึกษาในแอ่งโคราชคือเพื่อต้องการหาขอบเขต (ความลึก) ของชั้นเกลือหินในชุดหินมหาสารคาม ซึ่งได้มีผลกระทบต่อการสำรวจและพัฒนาน้ำบาดาล

ผลที่ได้จากการวิจัยระบุว่า ผิวบนของชั้นเกลือสามารถสะท้อนคลื่นเสียงกลับได้ดี แต่ไม่เสมอไปในทุกพื้นที่ คุณลักษณะการสะท้อนกลับเช่นนี้จะเห็นได้จากคลื่นปฐมภูมิและคลื่นทุติยภูมิ เพื่อที่จะแสดงความไม่สม่ำเสมอและความคลุมเครือของผลที่ได้นี้ ได้ทำการสร้างแบบจำลองของชั้นหินสามลักษณะเพื่อแสดงผลของการสะท้อนกลับของคลื่นที่เกิดขึ้น ผลที่ได้สรุปว่า ความคลุมเครือของผลที่ได้สามารถขจัดออกไปได้ด้วยการสำรวจคลื่นสั่นสะเทือนที่มีการควบคุมตัวแปรอย่างเหมาะสม

ABSTRACT

One of the main objectives of a seismic survey is to distinguish between different lithologies using the reflection of the waves at the interfaces of two layers. The amplitudes of these reflections depend mainly on the acoustic impedance of each layer (Z = density x velocity), but are defined by the reflection coefficient (R) at the interface between two layers, with

$$R = \frac{\rho_2 V_2 - \rho_1 V_1}{\rho_2 V_2 + \rho_1 V_1} = \frac{Z_2 - Z_1}{Z_2 + Z_1},$$

where 1 represents the upper and 2 the lower layer at the interface. Samples from different lithologies from the Khorat Basin in NE Thailand were used for laboratory measurements of density and seismic compressional and shear-wave velocities to investigate the origin of shallow seismic reflections. A main objective in the Khorat Basin is to identify the reflection of the top boundary of the rocksalt layer (Mahasarakham Formation), due to its impact on groundwater exploration and exploitation.

The results show that in many cases the top boundary of the salt layer produces a strong reflection at the interface with other lithologies, but not always. This applies in the same way for compressional as well as for shear-wave velocities. This ambiguity in the interpretation of seismic sections is illustrated with three synthetic seismograms using different lithological models. Finally, well control of seismic surveys is the best way to overcome these ambiguities in seismic data interpretation.

TABLE OF CONTENTS

LIST OF TABLES

LIST OF FIGURES

INTRODUCTION

Seismic surveys are the main tool for the examination of the subsurface. In the Northwest region of Thailand, especially in the Khorat Basin, shallow seismic data are used for groundwater exploration and exploitation (e.g. Satarugsa et al., 2000).

In general, the objective in seismic reflection surveys mainly is to map the depth, dip and strike of interfaces, which are usually parallel to the bedding. A second objective is to define stratigraphic variations from normal move-out measurements or from the amplitude and wave shape of reflection events (Sheriff, 1991). For an interpretation of such records the knowledge of the origin of the reflectivities is essential (see Johnston and Christensen, 1992).

In NE Thailand the rocksalt formation has a major influence on the groundwater system (see Satarugsa et al., 2000). Therefore one of the main targets is to detect the upper boundary of this layer by seismics. But the main problem is also to identify the reflection of this boundary in the seismic sections (see Satarugsa and Srisuk, 2000). This knowledge becomes more important in regions where subsurface structures changed the picture of the more or less horizontal layers, like salt domes, folds or solution caverns. These caverns, which are of natural occurrence or due to salt production, sometime can lead to hazardous sinkholes at the surface.

A base for an understanding of the reflectivity in seismic surveys can be laboratory measurements, where the conditions are known and defined. The essential physical rock properties are density and seismic velocities, together with a geological rock description. The rock samples can either come from outcrops or they can be cores of drilling (see Christensen and Szymanski, D.L., 1991; Dey-Barsukov et al., 2000).

METHODS AND MATERIAL

For this study most of the samples are taken from shallow outcrops in the greater Khorat area from Tertiary and Quaternary lithostratigraphic units, Upper Khorat Group and younger (see Boonser and Sonpirom, 1997). Additionally industrial '*body*' porcelain clay, already mixed with quartz and feldspar, was used to study the influence of water content on the physical properties of clay. This industrial clay has a similar composition than the natural clay, which can be found in Nakhon Ratchasima Province. Rocksalt samples of the Mahasarakham Formation (Upper Khorat Group, Upper Cretaceous) were taken from drilling holes, provided by the Asia Pacific Potash Corporation (Udon Thani).

The geological description of the samples, the composition and structure, was done macroscopically and by using a stereoscope.

Sample 1 *Location: Province Nakhon Ratchasima, District Khong; from a shallow outcrop.*

A reddish brown siltstone/claystone cemented with carbonate, similar like Sample 2 (see Figure 1a, b). The texture is less flaserlike than Sample 2, it looks more like bigger and smaller silt/clay lenses together. Clastic particles appear as less than mm small light grey and grey coloured grains. Parts of mm-sized black fissures indicate the existence of organic material. The sample shows several open cracks going through nearly the whole samples, probably due to drying shrinkage.

Sample 2 *Location: Province Nakhon Ratchasima, District Khong, from a shallow outcrop close to Sample 1.*

A reddish brown siltstone/claystone cemented with carbonate (Figure 1a). The texture is flaserlike indicated by different shades of the overall red colour. Clastic particles appear like in Sample 1. Parts of mm-sized black fissures indicate the existence of organic material. The sample shows many small open cracks throughout the sample, probably due to drying shrinkage like Sample 1.

Sample 3

Location:Province Nakhon Ratchasima, District Suranaree, from a shallow outcrop.

Sample 3 is a partly light grey, partly ochre and partly red coloured sandstone/ claystone (Figure 1b). The red parts mainly clay, whereas the other parts are sandier. Several mm-large single grains appear as well as black parts indicating organic material. Additionally plant stems, several mm long and up to two mm in diameter, are preserved in this sample, now entirely black coloured. The sample shows no depositional features like bedding or others, and compared to the other samples it is the most unconsolidated one.

Sample 4

Location: Province Nakhon Ratchasima, District Suranaree, from the same outcrop as Sample 3, but from the lithostratigraphic layer directly below.

A fine-grained siltstone with dark red colour (Figure 1b). The size of the grains is nearly equal and below 1 mm. The cement is a non-carbonate. The macroscopically investigations show really less clay content. The entire sample is homogenous showing no visible texture.

Sample 4z

Location: Province Nakhon Ratchasima, District Suranaree, from a shallow outcrop close to the one where Sample 3 and 4 were taken.

Macroscopically Sample 4z looks like Sample 4 (Figure 1c). It is also a fine-grained siltstone with dark red colour. Different from Sample 4 is the distinct carbonate cement and macroscopically visible small clay content.

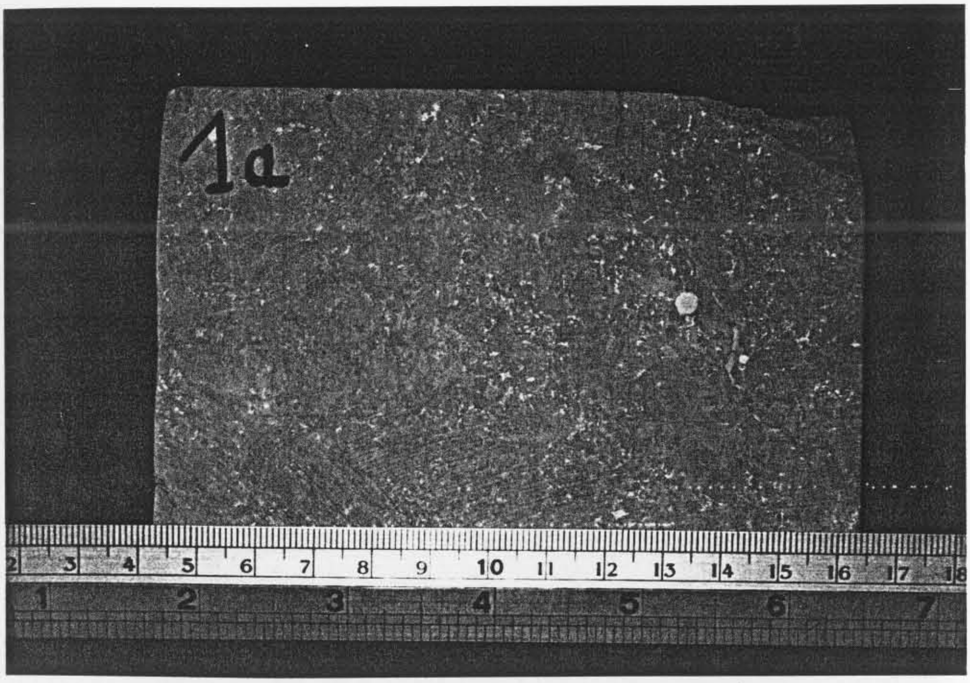

Figure 1a: **Top:** Sample 1 (specimen a), **bottom:** Sample 2 (specimen a), scale: white in cm, red in inch.

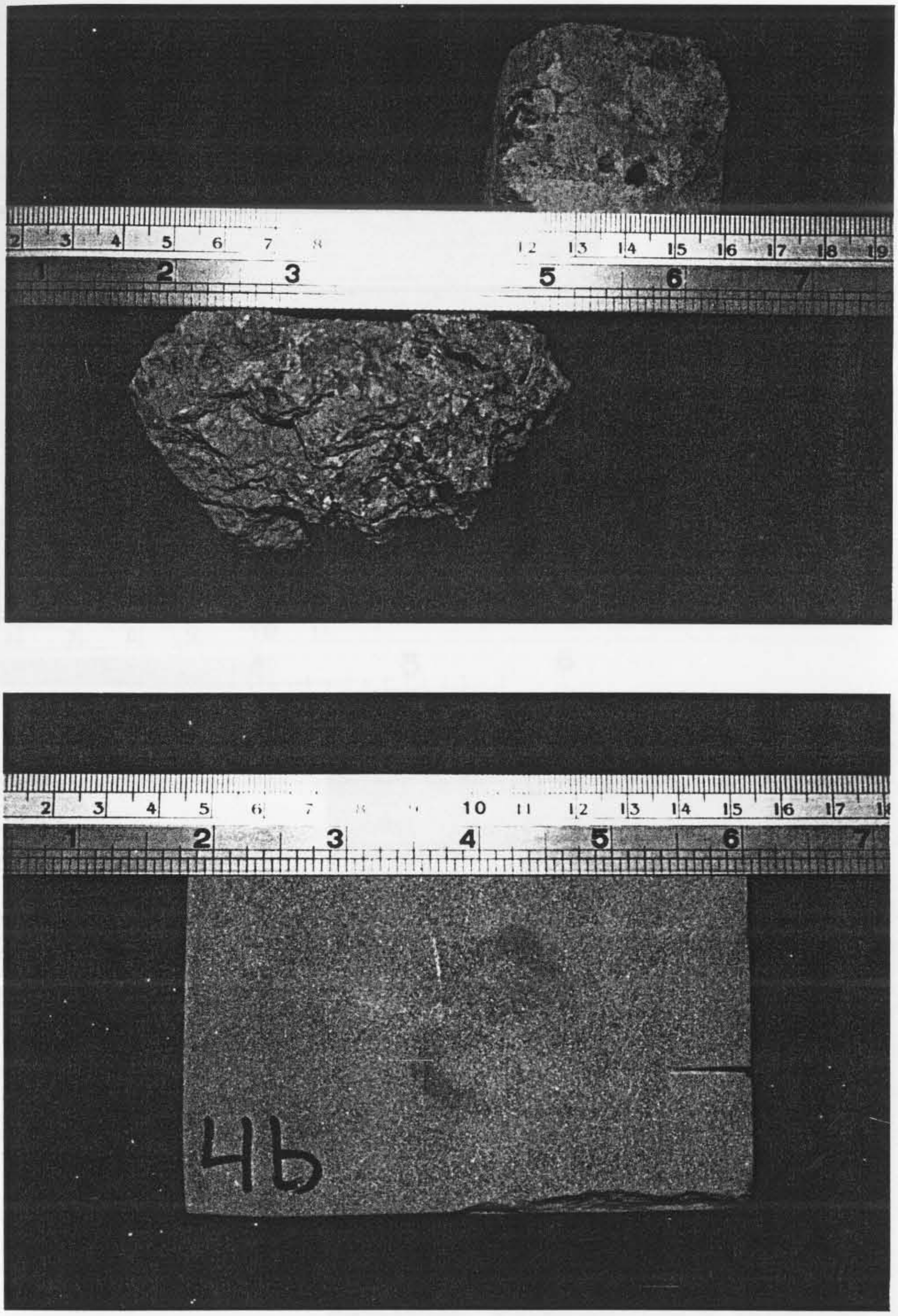

Figure 1b: **Top**: Sample 3, **bottom**: Sample 4 (specimen b),

scale: white in cm, red in inch.

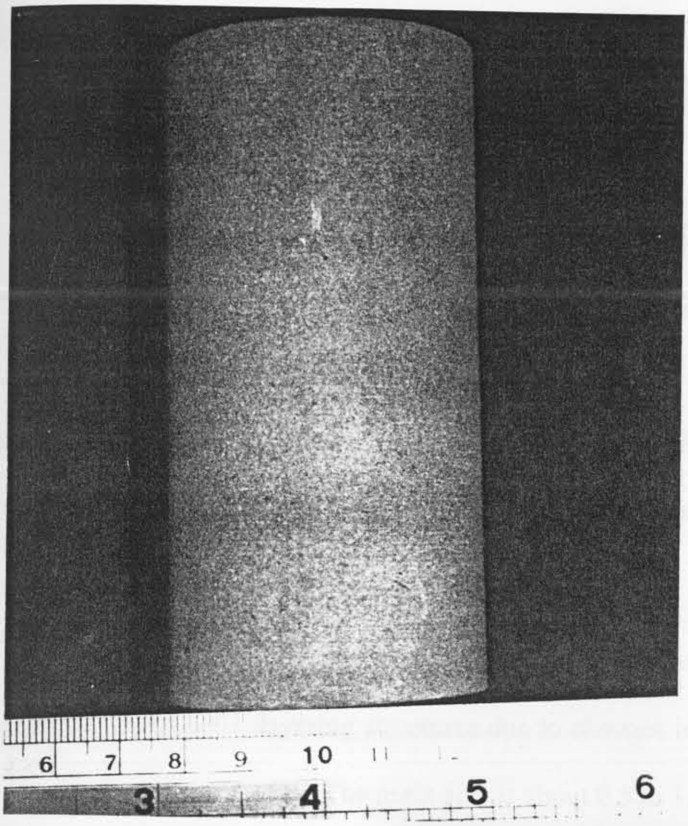

Figure 1c: **Top**: Sample 4z, **bottom**: Rocksalt sample (two specimens),

scale: white in cm, red in inch.

Clay Samples (dry, wet) *Location: from Central Ceramics International Ltd., Bangkok.*

The clay is industrial '*body*' porcelain clay, already mixed with quartz and feldspar (see Table 1). 'Wet' indicates the condition in which the clay is delivered from the company, whereas 'dry' specifies the condition after one week drying at room temperature.

Rocksalt Samples *Location: From Asia Pacific Potash Corporation, Province Udon Thani. Samples are from drilling holes, Mahasarakham Formation, probably the upper salt layer.*

Two different rocksalt samples were chosen (Figure 1c). Both show layering structures due to changes in the colour or/and in the presence of clay. The grain size is about 0.5 to 1.0 mm, partly larger.

Table1: Composition of the clay sample (*AI Common Porcelain Clay*), data from Central Ceramics International Ltd., Bangkok.

Compound	Test 1 [%]	Test 2 [%]	Test 3 [%]	Average [%]
Al_2O_3	22.377	22.072	22.400	**22.283**
SiO_2	64.463	64.483	64.728	**64.558**
CaO	0.198	0.203	0.205	**0.202**
Fe_2O_3	1.157	1.148	1.143	**1.149**
K_2O	3.483	3.585	3.558	**3.542**
MgO	0.308	0.571	0.365	**0.415**
Na_2O	0.668	1.073	0.600	**0.780**
TiO_2	0.197	0.187	0.186	**0.190**
MnO_2	0.028	0.031	0.031	**0.030**
P_2O_5	0.056	0.056	0.031	**0.048**

From each sample up to three different specimens with a geometric shape (cube or cylinder) were prepared for the determination of the physical properties. If a sedimentary layering was macroscopically visible the specimens were prepared in respect to it. Then the specimens were cut to a certain dimension, followed by a grinding and polishing of the cubic or cylindrical end faces. From dimension (length, diameter) and weight of the cylindrical or cubic specimens the bulk density (ρ_{bulk}) were calculated. Then for each specimen the traveltime of the P-wave and one shear-wave (usually the faster one) were determined with the Sonicviewer 170 (OYO Corporation). For the determination of the traveltime transducers with different frequencies were used: for V_P: 63 kHz, 200 kHz, 500 kHz and for V_S: 33 kHz and 100 kHz. From the traveltimes of the waves and the lengths of the samples the velocities can be calculated.

All these measurement were carried out at no confining pressure (tabletop measurements, see Figure 2). In shallow subsurface regions the confining pressure is comparably low and can be neglected. In similar studies for deeper regions confining pressure is becoming more important, there the seismic velocities in general increase with confining pressure (for example in hydrocarbon investigations; see Birch, 1960a,b; Schön, 1996).

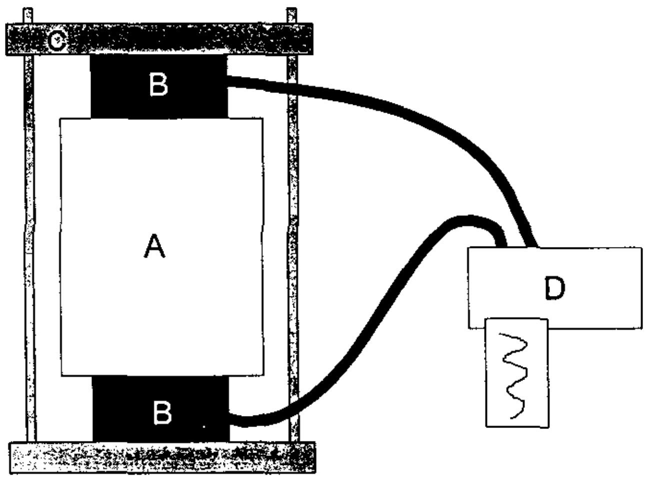

Figure 2: Schematic sketch of the configuration for the seismic tabletop measurements. **A**: sample (shape and size are varying), **B**: transducers (transmitter and receiver), **C**: holder device, **D**: Sonicviewer 170.

For the tabletop measurements a simple devise holding the transducers and the sample was made to ensure a good coupling between the sample and transducers and therefore ensure the same quality of all the seismic measurements. Figure 3 shows a time record from the Sonicviewer 170 for a rocksalt sample.

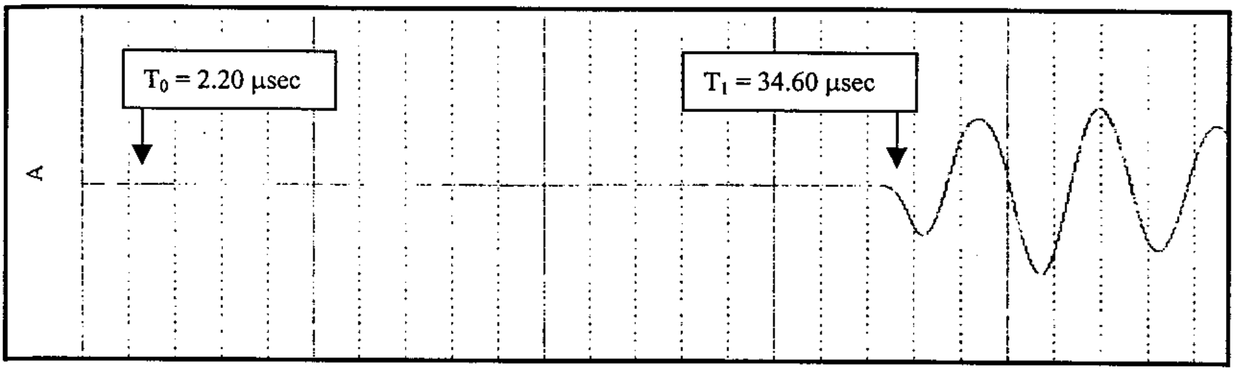

Figure 3: A time record from the Sonicviewer 170 from a rocksalt sample (length 143.66 mm) for a compressional wave measured with 200 kHz transducers. Time scale is 2 μsec per line. Low cut filter: 30 kHz ; High cut filter: 1000 kHz. T_o is the zero time for the equipment measured independently before. T_1 is the time the compressional wave travelled through the sample plus the zero time. The difference is the traveltime for the sample. From this and the sample length the wave velocity can be calculated (here 4.43 km/s).

From the laboratory data of the physical properties (bulk density, seismic velocities) the acoustic impedance (Z) were calculated for each sample using a mean value from the measurements of the different specimens from one sample. From this the reflection coefficient (R) can be determined for each interface between two lithologies. For a normal incident ray, the ratio of the amplitude of the reflected ray to the amplitude of the incident ray is given by

$$R = \frac{\rho_2 V_2 - \rho_1 V_1}{\rho_2 V_2 + \rho_1 V_1} = \frac{Z_2 - Z_1}{Z_2 + Z_1},$$

where $\rho_1 V_1$ and $\rho_2 V_2$ are the products of density and velocity - the acoustic impedance (Z) - above and below the interface separating two lithologies (layer 1 : top and layer 2 : bottom), respectively.

The acoustic impedance is a characteristic parameter for the lithology. The reflection coefficient, R, ranges from -1 to +1. If R= +1 or -1, all the incident energy is reflected, whereas if R = 0, all of the energy is transmitted. A negative value of R corresponds to a 180° phase change in the reflected wavelet (see Figure 4 and 5; also Sheriff, 1991; Johnston and Christensen, 1992).
The reflection coefficients based on laboratory measurements of the physical properties can be directly used for the understanding of reflectivity in seismic surveys in areas with less stratigraphic control (e.g. Christensen and Szymanski, 1991).

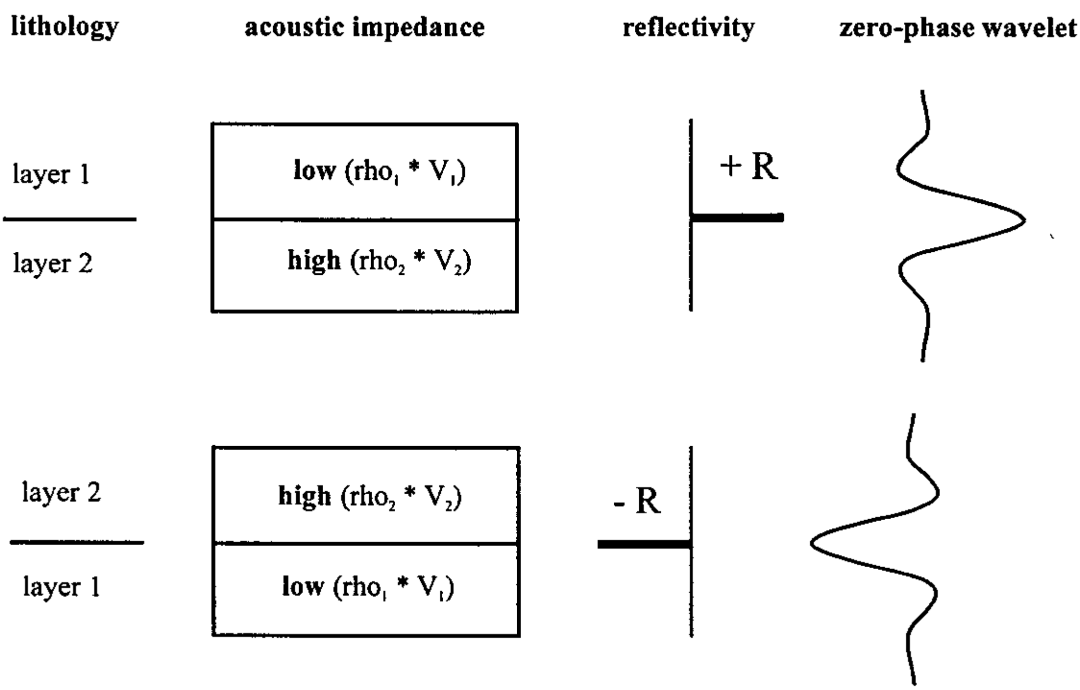

Figure 4: Low to high and high to low acoustic impedance contrasting interfaces between layer 1 and layer 2 with the theoretical reflection response (reflectivity) and a schematic zero-phase wavelet from a seismic survey.

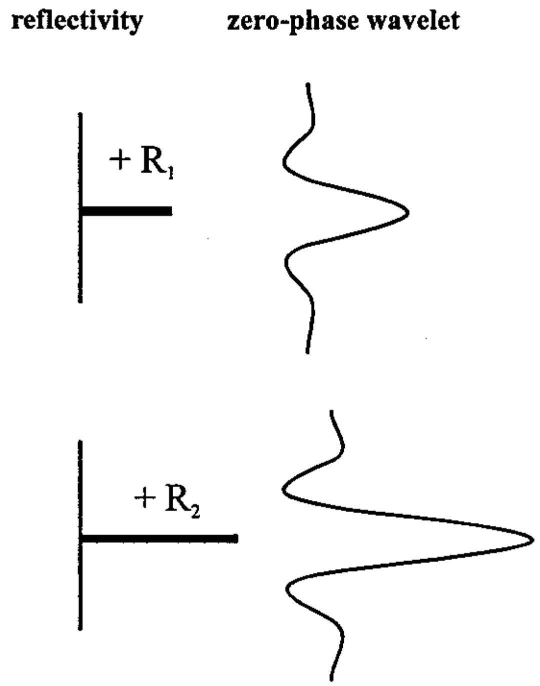

Figure 5: The relationship between a theoretical reflection response (reflectivity) and a schematic zero-phase wavelet from a seismic survey, with $R_2 > R_1$.

RESULTS AND DISCUSSION

The results of the laboratory measurements are presented in Table 2 and 3. The data of the bulk densities, the compressional and shear-wave velocities are average values from measurements on different specimens from the same sample (see Appendix). A possible influence of the transducer frequencies on the travel time can be considered smaller than the overall measurement error. Additionally, data for saltwater and anhydrite were taken from the literature (see Table 2 and 3).

The velocity data are in general consistent with published data (see for example Gebrande, 1982; Schön, 1996). Furthermore, the laboratory derived compressional wave velocity data for the rocksalt (4.45 km/s) are in good agreement with values from pervious seismic surveys in Northeast Thailand (4.5 km/s, Satarugsa and Srisuk, 2000). The value for the overburden published in the same paper with V_P = 1.65 km/s is only about 150 m lower than the average value for the Samples 1, 2, 3, 4, 4z, clay-wet and clay-dry (1.79 km/s) of this study. But the velocity data from these seven samples show a variation from 1.27 km/s (Sample 3) to 2.28 km/s (Sample 4z).

For the clay samples the P-wave velocities decrease from wet to dry condition, whereas the shear-wave velocities increase. This in accordance with previous investigations (e.g. Elliot and Wiley, 1975, Hübner et al., 1985) and theoretical studies (e.g. Domenico, 1977), although the decrease in V_S is higher than expected.

From the velocity and density data the acoustic impedance values were calculated. Anhydrite shows the highest value for V_P (16.65 $*10^6$ kg/m^{2}s), due to the highest compressional wave velocities, followed by rocksalt with 9.52 $*10^6$ kg/m^{2}s. The other samples have values about 5 $*10^6$ kg/m^{2}s and below. The shear-wave acoustic impedance data show a similar picture, rocksalt (5.26 $*10^6$ kg/m^{2}s) has the highest value, whereas the other samples have values about 3.5 $*10^6$ kg/m^{2}s and lower.

Table 2: Laboratory data of bulk density, V_P and V_S. Anhydrite data are from Gebrande (1982). Saltwater data: density from Schlumberger (1989); V_P from Wyllie et al. (1956).

Sample	Density	V_P	V_S
No.	[g/cm^3]	[km/s]	[km/s]
1	2.36	2.17	1.47
2	2.28	2.23	1.54
3	1.77	1.27	0.77
4	2.18	1.54	1.01
4z	2.34	2.28	1.50
clay-wet	2.01	1.58	0.50
clay-dry	1.90	1.45	1.21
anhydrite*	2.96	5.62	-
saltwater*	1.15	1.70	-
rocksalt	2.14	4.45	2.46

Table 3: Acoustic impedance values calculated from the laboratory and literature data of bulk density, V_P and V_S (see Table 2).

	V_P	V_S
sample no.	**acoustic impedance [*10^6 kg/m²s]**	**acoustic impedance [*10^6 kg/m²s]**
1	5.12	3.47
2	5.08	3.51
3	2.25	1.36
4	3.36	2.20
4z	5.34	3.51
clay-wet	3.18	1.01
clay-dry	2.76	2.30
anhydrite*	16.65	-
saltwater*	1.95	-
rocksalt	9.52	5.26

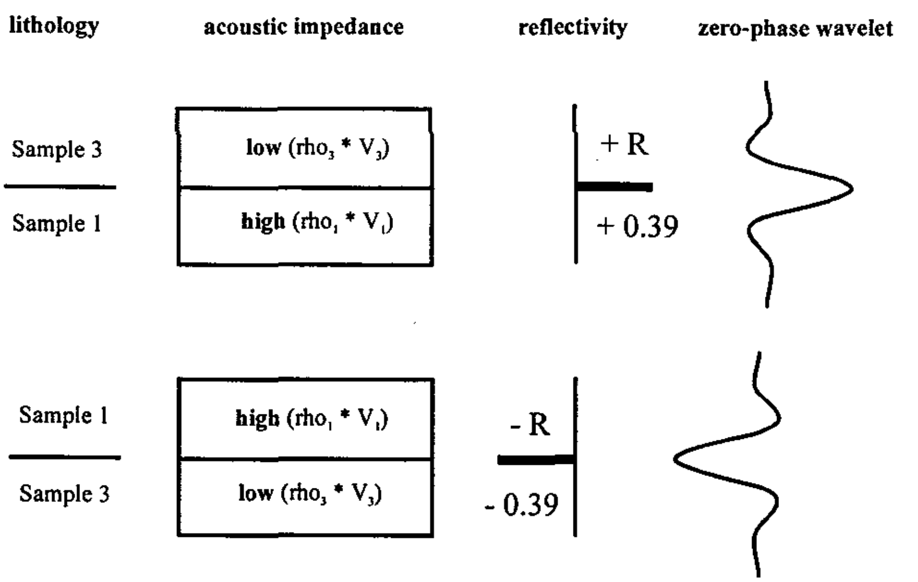

Figure 6: **Top:** Low to high acoustic impedance contrasting interface between Sample 3 and Sample 1 with the theoretical reflection response (reflectivity value: +0.39) and a schematic zero-phase wavelet from a seismic survey. **Bottom:** A high to low acoustic impedance contrast interface between Sample 1 and Sample 3 with the theoretical reflection value of -0.39 and a schematic zero-phase wavelet from a seismic survey.

The data from the laboratory measurements were taken to calculate the reflectivity values for all possible situations above the rocksalt formation. For example, Sample 1 can represent the top layer and Sample 3 the bottom layer, with a reflectivity of -0.39 (see Figure 6). In the other way Sample 3 is the top layer and Sample 1 is the bottom layer. The resulting reflectivity is 0.39; the same value like in the first example, but the opposite sign (see Figure 6).

Reflectivity from compressional waves

For the compressional waves the highest reflectivity values were mainly found at the interfaces where the top or bottom layer is rocksalt or anhydrite, due to the high acoustic impedance data of both rock types (see Table 3). For the detection of rocksalt layers in seismic surveys the reflectivity values are important where rocksalt is the bottom layer at the interface. For this situation the reflectivity values are relatively high (R about +0.5 to +0.6) for the majority of the top layers, like Sample 3, Sample 4, clay-wet, clay-dry and saltwater (see Table 4). Therefore the identification of the 'top rocksalt interface' (= upper boundary of the rocksalt formation) will be relatively simple, because this interface will produce a strong reflection in the seismogram with a large amplitude.

Table 4: Calculated reflectivity values for the compressional wave velocities for all possible situations above the rocksalt layer using the data from Table 2 and 3.

		top layer								
	samples	**1**	**2**	**3**	**4**	**4z**	**clay-wet**	**clay-dry**	**salt-water**	**anhydrite**
bottom layer	**1**		0.00	**0.39**	0.21	-0.02	0.23	**0.30**	0.45	-0.53
	2	0.00		**0.39**	0.20	-0.02	0.23	**0.30**	0.45	-0.53
	3	-0.39	-0.39		-0.20	-0.41	-0.17	-0.10	0.07	-0.76
	4	-0.21	-0.20	0.20		-0.23	0.03	0.10	0.27	-0.67
	4z	0.02	0.02	**0.41**	0.23		0.25	**0.32**	0.47	-0.52
	clay-wet	-0.23	-0.23	0.17	-0.03	-0.25		0.07	0.24	-0.68
	clay-dry	-0.30	-0.30	0.10	-0.10	-0.32	-0.07		0.17	-0.72
	salt-water	-0.45	-0.45	-0.07	-0.27	-0.47	-0.24	-0.17		-0.79
	anhydrite	0.53	0.53	0.76	0.67	0.52	0.68	0.72	0.79	
	rocksalt	**0.30**	**0.30**	**0.62**	**0.48**	**0.28**	**0.50**	**0.55**	**0.66**	-0.27

For the situation that Sample 1, Sample 2 or Sample 4z will be the top layer at the interface to the lower rocksalt the reflectivity values will be only about +0.3 (see Table 4). In this case, the interface of the 'top rocksalt' produces a reflectivity, which is (only) as strong as the reflectivity at the interface between Sample 3—Sample 1 (+0.39) or Sample 3—Sample 2 (+0.39), or clay-dry—Sample 1 (+0.30), clay-dry—Sample 2 (+0.30) or clay dry—Sample 4z (+0.32), with top layer—bottom layer (reflectivity). The magnitudes of the reflection coefficients at these interfaces are nearly the same and the signs are equal. Therefore the identification of the 'top rocksalt interface' becomes more ambiguous, which makes the interpretation and the use of seismograms more difficult.

Synthetic seismograms are used to show the ambiguity and difficulty of the seismic data interpretation (Figure 7). Three different models were used. The input data for each model are shown in Table 5. From this data a ricker wavelet with a 30 Hz frequency was generated using a simple reflectivity algorithm, without transmission (compare Christensen and Szymanski, 1991).

In the first model the interface between clay-wet and the rocksalt leads to strong reflectivity ($R = +0.55$), which can be clearly identified in the seismogram by the high amplitude (see Satarugsa and Srisuk, 2000). In the second model the clay-wet layer was replaced by Sample 4z. The reflection at this interface is not strong like in the first model due to the low reflection coefficient of +0.28 (see Table 4). This reflection cannot be clearly identified anymore in comparison to the other reflections in this synthetic seismogram. In the third model rocksalt was replaced by Sample 1 with Sample 3 as the top layer. This interface produces a strong reflection due to $R = 0.39$. This strong reflection may be misinterpreted as the top of the rocksalt formation like in the synthetic seismogram of Model 1.

Table 5: Synthetic seismograms: Input data for the different models, using the bulk density and velocity data from the laboratory measurements.

Model 1			
density [g/cm^3]	**relative thickness**	**V_P [km/s]**	**lithology**
2.28	0.02	2.23	Sample 2
1.77	0.02	1.27	Sample 3
2.18	0.04	1.54	Sample 4
2.01	0.04	1.58	clay-wet
4.45	0.08	2.14	rocksalt
2.28	0.02	2.23	Sample 2

Model 2			
density [g/cm^3]	**relative thickness**	**V_P [km/s]**	**lithology**
2.28	0.02	2.23	Sample 2
1.77	0.02	1.27	Sample 3
2.18	0.04	1.54	Sample 4
2.34	0.04	2.28	Sample 4z
4.45	0.08	2.14	rocksalt
2.28	0.02	2.23	Sample 2

Model 3			
density [g/cm^3]	**relative thickness**	**V_P [km/s]**	**lithology**
2.28	0.02	2.23	Sample 2
1.77	0.02	1.27	Sample 3
2.18	0.04	1.54	Sample 4
1.77	0.04	1.27	Sample 3
2.36	0.08	2.17	Sample 1
2.28	0.02	2.23	Sample 2

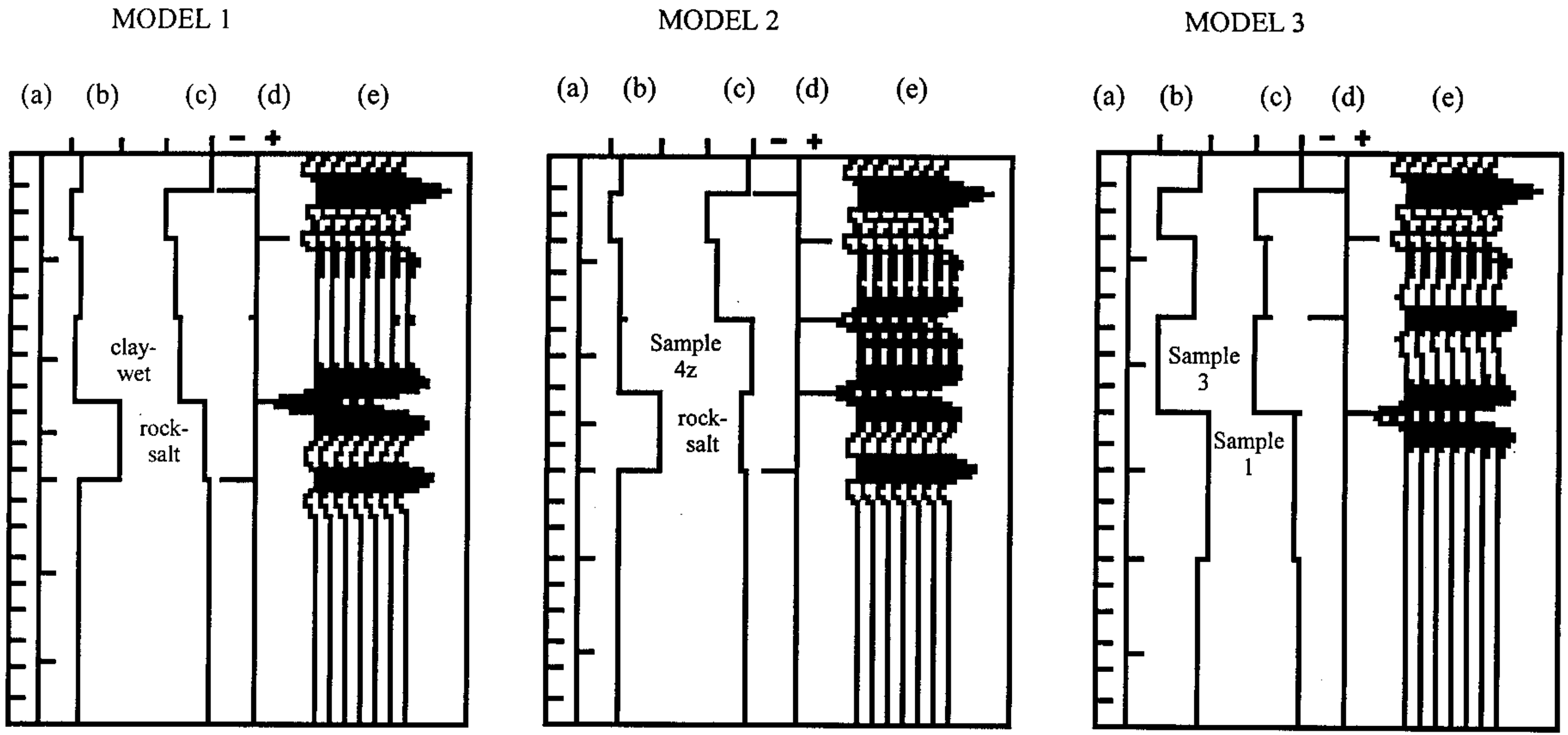

Figure 7: Synthetic seismograms for three different situations (models),

(a) relative depth, (b) density, (c) V_P, (d) reflectivity and (d) synthetic seismogram with 7 traces (data in Table 5).

(Note: Orientation between wave amplitudes and reflectivity coefficient is reverse in comparison to the previous figures.)

Reflectivity from shear-waves

The calculations of the reflection coefficients for the shear-wave velocities show a similar situation like the compressional wave velocities (see Table 6). The highest R-values are at the interface where rocksalt is the bottom layer (e.g. Sample 3 or clay-wet as the top layer). But relatively high reflection coefficients are produced at many interfaces where rocksalt is neither bottom nor top layer, e.g. clay-wet—Sample 4z.

Table 6: Calculated reflectivity values for the shear wave velocities for all possible situations above the rocksalt layer using the data from Table 2 and 3.

	top layer							
Bottom Layer	**samples**	**1**	**2**	**3**	**4**	**4z**	**Clay-wet**	**clay-dry**
	1		-0.01	**0.44**	0.22	-0.01	**0.55**	0.20
	2	0.01		**0.44**	0.23	0.00	**0.55**	0.21
	3	-0.44	-0.44		-0.24	-0.44	0.15	-0.26
	4	-0.22	-0.23	0.24		-0.23	0.37	-0.02
	4z	0.01	0.00	**0.44**	0.23		**0.55**	0.21
	clay-wet	-0.55	-0.55	-0.15	-0.37	-0.55		-0.39
	clay-dry	-0.20	-0.21	0.26	0.02	-0.21	**0.39**	
	rocksalt	0.21	0.20	**0.59**	**0.41**	0.20	**0.68**	**0.39**

Therefore additional shear-wave surveys will not provide more data to overcome the ambiguity in the interpretation of V_P seismograms (see above). However, shear-wave surveys are much more expensive than compressional wave surveys and so usually not used in groundwater investigation efforts.

CONCLUSIONS

Seismic surveys are the main tool for the examination of the subsurface, but the interpretation of the seismograms still remains ambiguous, especially for the identification of different lithologies. The calculated reflectivity coefficients based on laboratory derived bulk density and velocity values from NE Thailand show that different lithologies can produce a similar reflection at an interface. This applies in the same way for compressional as well as for shear-wave velocities.

Therefore seismic surveys need well control. This means, that the reflections in a seismogram have to be confirmed by well data where the lithology is know either from cuttings or from cores. This is also necessary for shallow seismic survey in groundwater investigations and not only for deep seismic survey in hydrocarbon exploration. For the Khorat Basin in NE Thailand the wells for groundwater exploitation can be used for this correlation. The experiences gathered from a few well sites then can be used in the interpretation of future seismic surveys.

REFERENCES

Birch, F., 1960a, The velocity of compressional waves in rocks to 10 kilobars. Part I: J. Geophys. Res., 65: 1083-1102.

Birch, F., 1960b, The velocity of compressional waves in rocks to 10 kilobars. Part II: J. Geophys. Res., 66: 2199-2224.

Boonsener, M. and Sonpirom, K., 1997. Correlation of tertiary rocks in Northeast Thailand. Proceedings of the Int. Conference on 'Stratigraphy and tectonic evolution of Southeast Asia and the South Pacific', 19-24 Aug 1997, Vol. 2: 656-661.

Christensen, N.I. and Szymanski, D.L., 1991. Seismic properties and the origin of reflectivity from a classic Paleozoic sedimentary sequence, Valley and Ridge province, southern Applachians. Geol. Soc. Am. Bull., 103: 277-289.

Dey-Barsukov, S., Dürrast, H., Rabbel, W., Siegesmund, S., and Wende, S., 2000, Aligned fractures in carbonate rocks: Evidence from laboratory and in situ measurements of seismic anisotropy. Int. J. Earth Sciences, 88:829-839.

Domenico, S.N., 1977, Elastic properties of unconsolidated porous sand reservoirs. Geophysics, 42: 1339-1368.

Elliot, S.E. and Wiley, B.F., 1975, Compressional wave velocities of partially saturated, unconsolidated sands. Geophysics, 40: 949-954.

Gebrande, H., 1982, Elastic wave velocities and constants of elasticity of rocks and rock forming minerals, in G. Angenheister, , Ed., Physical properties of rocks: Landolt-Börnstein, V/1b, Springer-Verlag, 1-140.

Hübner, S., Meissner, R. and Stümple, H., 1985, Einflüsse lithologischer Parameter oberflächennaher Sedimente auf Kompressions- und Scherwellengeschwindigkeiten. In: Heitfeld, K.-H., Ingenieurgeologische Probleme im Grenzbereich zwischen Locker- und Festgesteinen. Springer Publisher, Berlin.

Johnston, J.E. and Christensen, N.I., 1992. Shear wave reflectivity, anisotropies, Poisson's ratios, and densities of a southern Appalachian Paleozoic sedimentary sequence. Tectonophysics, 210: 1-20.

Satarugsa, P. and Srisuk, K., 2000, Applied geophysics solving the hydrogeological problems in the Northesast, Thailand. J. Geol. Soc. Thailand, 1: 19-26.

Satarugsa, P., Virasri, R., Navawitphaisith, S., Chotrasri, O., 2000, Evaluation of geophysical investigations for rapid mapping of the rock salt in the Maha Sarakham Formation in Northeast Thailand. Proc. Internat. Conf. Applied Geophysics, 9-10 Nov. 2000, Chiang Mai, Thailand, 39-52.

Schlumberger, 1989, Log interpretation: Principles/Applications: Schlumberger Educational Service.

Schön, J.H., 1996, Physical properties of rocks: Fundamentals and principles of petrophysics: Pergamon.

Sheriff, R.E., 1991, Encyclopedic dictionary of exploration geophysics: Geophysical Reference Series No.1, SEG.

Wyllie, M.R.J., Gregory, A.R. and Gardner, L.W., 1956, Elastic wave velocities in heterogeneous and porous media: Geophysics, 21, 41-70.

APPENDIX

Laboratory data:

Sample Specimen	Transducer frequency $P=V_P/S=V_S$	Sample Length mm	Traveltime To microsec	Traveltime T1 microsec	Velocity km/s		Mean Velocity km/s
1a	63kHz;P	121.00	1.7	60.0	2.08	V_P	
1b	63kHz;P	85.80	1.7	42.4	2.11	V_P	
1c	200kHz;P	78.10	2.0	36.0	2.30	V_P	
1c	63kHz;P	78.10	1.7	37.0	2.21	V_P	**2.17**
1b	100kHz;S	85.80	1.8	60.0	1.47	V_S	**1.47**
2a	500kHz;P	74.90	0.9	35.0	2.20	V_P	
2a	500kHz;P	61.80	0.9	28.0	2.28	V_P	
2b	500kHz;P	24.10	0.9	11.4	2.30	V_P	
2c	63kHz;P	72.50	1.7	35.2	2.16	V_P	**2.23**
2a	100kHz;S	61.80	1.8	43.6	1.48	V_S	
2a	100kHz:S	74.90	1.8	54.0	1.43	V_S	
2c	100kHz;S	72.50	1.8	44.0	1.72	V_S	**1.54**
3a	200kHz;P	41.70	2.0	32.0	1.39	V_P	
3a	500kHz;P	41.70	0.9	34.0	1.26	V_P	
3b	63kHz;P	79.50	1.7	70.0	1.16	V_P	**1.27**
3a	100kHz;S	41.70	1.8	59.0	0.73	V_S	
3b	100kHz;S	79.50	1.8	100.0	0.81	V_S	**0.77**
4a	500kHz;P	55.90	0.9	37.2	1.54	V_P	
4a	500kHz;P	104.00	0.9	69.0	1.53	V_P	
4b	500kHz;P	78.00	0.9	48.0	1.66	V_P	
4b	500kHz;P	88.00	0.9	63.2	1.41	V_P	
4c	500kHz;P	16.50	0.9	11.6	1.54	V_P	**1.54**
4a	100kHz;S	55.90	1.8	56.0	1.03	V_S	
4a	100kHz;S	104.00	1.8	105.0	1.01	V_S	
4b	100kHz;S	78.00	1.8	76.8	1.04	V_S	
4c	100kHz;S	16.50	1.8	19.0	0.96	V_S	**1.01**

Sample Specimen	Transducer frequency P=Vp/S=Vs	Sample Length mm	Traveltime To microsec	Traveltime T1 microsec	Velocity kHzm/s		Mean Velocity km/s
Clay-wet	P 63kHz	14.90	2.1	11.0	1.67	V_P	
		12.35	2.1	10.0	1.56	V_P	
		14.00	2.1	11.0	1.58	V_P	
		14.10	2.1	11.6	1.48	V_P	
		14.50	2.1	11.0	1.63	V_P	
		17.60	2.0	14.8	1.38	V_P	
		14.80	2.0	10.8	1.68	V_P	
		14.10	2.0	10.7	1.62	V_P	**1.58**
Clay-wet	S 33kHz	6.60	2.5	15.8	0.50	V_S	
		7.20	2.5	16.4	0.52	V_S	
		8.10	2.5	16.8	0.57	V_S	
		5.70	2.5	15.8	0.43	V_S	**0.50**
Clay-dry	P 63kHz	43.00	2.0	32.2	1.42	V_P	
		42.90	1.85	31.2	1.46	V_P	
		42.90	1.85	30.6	1.49	V_P	
		42.90	1.85	30.8	1.48	V_P	
		42.90	1.85	31.6	1.44	V_P	
		42.90	1.85	32.0	1.42	V_P	**1.45**
Clay-dry	S 33kHz	43.00	2.1	38.8	1.17	V_S	
		43.00	2.1	37.6	1.21	V_S	
		43.00	2.1	36.6	1.25	V_S	
		42.90	2.5	38.4	1.19	V_S	
		42.90	2.5	38.0	1.21	V_S	**1.21**
4z	P 63 kHz	107.25	1.80	48.8	2.28	V_P	**2.28**
		107.25	2.70	74.0	1.50	V_S	**1.50**
Salt	P200kHz	143.60	2.20	34.6	4.43	V_P	
	P200kHz	146.30	2.20	35.0	4.46	V_P	**4.45**
	S100kHz	143.60	1.80	60.6	2.44	V_S	
	S100kHz	146.30	1.8	60.8	2.48	V_S	**2.46**

CURRICULUM VITAE

Principal investigator

Name :	Helmut Duerrast
Present Position :	Lecturer
Present address :	School of Geotechnology Institute of Engineering Suranaree University of Technology 111 University Avenue, Muang District Nakhon Ratchasima 30000 THAILAND

Education :

Postdoctoral Fellow	University of Göttingen/Germany, and University of Madison-Wisconsin/U.S.A.	1998-2000
Ph.D. in Natural Sciences (Dr. rer. nat.)	University of Göttingen/Germany	1997
Diploma in Geology/Palaeontology (Dipl. Geol./Palaeont.)	University of Göttingen/Germany, and University of Münster/Germany	1993

Research Fields :	Applied Geology and Geophysics, Hydrogeophysics, Petrophysics, Anisotropy, Structural Geology

Peer-reviewed Publications:

1. Dürrast, H., Jahns, E., Tischer, A., Siegesmund, S., 2001, Preferred orientation of microcracks created during triaxial compressional experiments using Piesberger Sandstein samples. Z. dt. geol. Ges., 152/2-4: 611-620 (in German, with English abstract).
2. Dey-Barsukov, S., Dürrast, H., Rabbel, W., Siegesmund, S. and Wende, S., 2000. Aligned fractures in carbonate rocks: Evidence from laboratory and in situ-measurements of seismic anisotropy. Int. Journ. Earth Sciences (Geol. Rundschau), 88/4: 829-839.
3. Dürrast, H. and Siegesmund, S., 1999. Correlation between rock fabrics and petrophysical properties of carbonate rocks. Int. Journ. Earth Sciences (Geol. Rundschau), 88/3: 392-408.
4. Dürrast, H., Siegesmund, H. and Prasad, M., 1999. Structural damage evaluation of natural building stones: Potential and limitations of ultrasonic diagnosis. Z. dt. geol. Ges., 150/2, 359-374 (in German, with English abstract).
5. Vollbrecht, A., Dürrast, H., Kraus, J. and Weber, K., 1994. Paleo-stress directions deduced from microcrack fabrics in KTB core samples and exposed granites from the surrounding field. Scientific Drilling, 4: 233-241.
6. Siegesmund, S., Vollbrecht, A., Nover, G., Dürrast, H., Müller, J. and Weber, K., 1993. Fabric controlled anisotropy of petrophysical properties observed in KTB core samples. Scientific Drilling, 4: 31-54.